Astrocytic IGF-1 and IGF-1R Orchestrate Mitophagy in Traumatic Brain Injury

Ren Dabin
Department of Neurosurgery, Shanghai Pudong New area People's Hospital, Shanghai, China
Chen Wei
Department of Neurosurgery, Shanghai East Hospital, Tongji University School of Medicine, Shanghai, China
Shu Liang
Department of Neurology, Shanghai Ninth People's Hospital,Shanghai, China
Cao Ke
Department of Neurosurgery, Shanghai Pudong New area People's Hospital, Shanghai, China
Wang Zhihan
Department of Neurosurgery, Shanghai Pudong Hospital affiliated to Fudan University, Shanghai, China
Ping Zheng (jojo_ras@126.com)
Department of Neurosurgery, Shanghai Pudong New area People's Hospital, Shanghai, China

Research article

Keywords: Astrocyte, IGF-1, IGF-1R, Dcp2,mitophagy, cognition, traumatic brain injury

Posted Date: August 10th, 2020

DOI: https://doi.org/10.21203/rs.3.rs-41602/v1

Abstract

Background

Defective brain hormonal signaling and autophagy have been associated with neurodegeneration after brain insults, characterized by neuronal loss and cognitive dysfunction. However, less studies have link them in the context of brain injury. Insulin like growth factor-1 (IGF-1) is an important hormone that contributes to growth, cell proliferation and autophagy, also expressed in the brain.

Methods

We applied proteomics to investigate the role of astrocytic IGF-1 in TBI and related neuroprotective mechanisms.

Results

We found reduced plasma IGF-1 is correlated with cognition in TBI patients. Overexpression of astrocytic IGF-1 improves cognitive dysfunction in TBI mice and cocultured astrocytes prevent neuronal excitotoxicity with IGF-1 pathway dependent. At the molecular level, proteomics data show IGF-1 related NF-kB pathway transcriptionally regulates decapping mRNA2 (Dcp2) and miR-let-7, together with IGF-1R to orchestrate mitophagy in TBI. Finally, we demonstrate that TBI induces impaired mitophagy at the chronic stage and IGF-1 treatment could facilitate the mitophagy marker.

Conclusion

By showing that IGF-1 is an important mediator of the beneficial effect of neural-endocrine network in TBI models, our findings place IGF-1/IGF-1R as a potential target capable of non-coding RNAs and opposing mitophagy failure and cognition impairment in TBI.

Background

Traumatic brain injury (TBI) is a common and disabling disease causing severe disability worldwide in 150 to 200 million people annually[1]. Many more suffer long-term cognitive and psychological problems with variable natural history[2]. One of the major pathological hallmarks of TBI is phosphorylated tau [3, 4], which results in poor clinical outcomes after TBI. We currently showed that both pharmaceutically targeting tau phosphorylation or genetic manipulation of tau could prevent cognition dysfunction after experimental TBI [5]. However, there are currently no drug treatments available to improve cognition or promote its recovery in clinical session and it is unclear which factor contributes to the cognitive recovery after TBI as well.

One potential factor might be post-traumatic hypopituitarism, which can be triggered by TBI and influence brain repair [6, 7]. Insufficiency of growth factor (GH) is considered the major risk factor for TBI outcome and insulin like growth factor-1 (IGF-1) is a direct downstream of GH [8]. GH replacement in TBI increases serum IGF-I and improves attention, memory, and psychological well-being [9]. Variations in serum IGF-I concentrations have been related to brain structure and cognitive function [10]. We previously demonstrate that astrocytic IGF-1 can prevent excitotoxicity in neurons and regulate the expression of GSK-3β, one kinase for tau phosphorylation and thereby reducing the hyperphosphorylated tau.

IGF-1 has shown to increase the mitophagy via activating AMPK signal [11]. We have shown mitophagy is impaired in the chronic stage of TBI [12, 13], and accordingly we predict that this might be due to the lower IGF-1 status after TBI, as tau phosphorylation can disrupt the mitophagy [14]. We also find astrocytes have a supporting role for neurons and protect against excitotoxic injury with IGF-1 dependent [15, 16]. We and others have demonstrated astrocytic upregulation of IGF-1 after brain injury can also improve neurological outcomes in animal models via decreasing phosphor-tau levels[17]. Although a series of studies have applied IGF-1 in brain insults like stroke and TBI, the clinical application is limited due to its adverse effects found in animal studies. Therefore, it is important to explore the potential mechanisms in IGF-1 treated animals to identify new targets. And the relationship between mitophagy and tau in TBI session remains elucidated.

Here, we applied proteomics to study the therapeutic mechanisms in astrocytic IGF-1 after brain insults and further link the downstream pathway with mitophagy and neurological outcome. Therefore, we hypothesized that IGF-1 status would impact recovery after TBI such that improvement in mitophagy and cognitive measures.

Methods

Patients and serum IGF-1 status

Human blood samples were obtained for analysis from TBI patients recruited in Department of Neurosurgery at Shanghai Pudong New area People's Hospital with institutional approval from Ethics Review Board (Ethics No. 2170063) from Jan 2019 to Jul 2019. 2–3 ml of venous blood from TBI was collected at 8am on 3days after injury and stored at -80 °C until analysis. Absolute IGF-I was tested by radio autoimmuno assay as previously reported [8]. Patients were then assigned to groups with different brain severity (Glasgow Coma Scale, GCS), neurological outcome (Glasgow Outcome Scale, GOS) and cognition scores (Montreal Cognition Assessment, MoCA), respectively, to identify the relationship between IGF-1 and these parameters. To account for the finding that IGF-I level declines naturally with age, the groups were age-matched. There are no statistical differences regarding the basic characteristics of patients and healthy controls (age, gender, education background, data not shown). Blood collection and clinical data from all patients were obtained from their relatives with the consent form.

Cognition assessment

Patients underwent a MoCA testing previously found to be sensitive to impairments after TBI at six months post injury [18, 19] [20]. All TBI patients were assess at 6 months post injury in our study as well. The total score of MoCA is 30 points and cognitive dysfunction is indicated by less than 26. The item of MoCA includes visuospatial and executive functioning, naming, attention and calculation, language, abstraction, delayed recall and orientation.

Reagents and antibodies

The rabbit polyclonal antibody pS356, which recognized phospho-tau at Ser356 was purchased from Abacm (ab92682). The mouse monoclonal antibody NeuN, which recognized neurons in the brain, was also purchased from Abcam (ab104224). The rabbit polyclonal anti-Dcp2 (ab28658) and mouse monoclonal anti-IGF-1R (ab16890) were purchased from Abcam. Rabbit polyclonal to ATG8 (ab4753), mouse monoclonal to Atg5 (ab238092), rabbit polyclonal to ATG14L (ab227849), rabbit monoclonal [EPR19662] to Beclin 1, rat monoclonal [1D4B] to LAMP1 (ab25245) and mouse monoclonal to SQSTM1 / p62 - Autophagosome Marker (ab56416) were used to assess the mitophagy level in cultured cells. Mouse monoclonal [HM-2] to MAP2 (ab11267) and rabbit monoclonal [EPR16778] to beta-Tubulin(ab201831)were used to evaluate the neuronal growth situation in-vitro. Rat BNIP3(ab10433,abcam) and PINK1(23274-1-AP□proteintech) were used for mitophagy assessment in TBI mice; Mouse monoclonal [mAbcam 8226] to beta Actin was used as loading control (ab8226).Bicinchoninic acid protein assay kit (BCA kit) was purchase from Pierce Biotechnology. Enhanced chemiluminescence detection kit was purchased from GE healthcare. AG1024 (121767) was purchased from Sigma-Aldrich in the InhibitorSelect IGF Signaling Pathway Inhibitor Panel (407249, Sigma-Aldrich). General chemicals, such as sodium deoxycholate (DOC), sodium dodecyl sulphate (SDS) and IGEPAL CA-630 (NP-40), were purchased from Sigma-Aldrich. LY294022 (#9901), an inhibitor of phosphatidyl- inositol 3-kinase (PI3K) and SB203580 and p38 MAPK inhibitor(#5633), were purchased from Cell Signaling Technology. MG-132, Nfkb1 inhibitor (#474790), was purchased from Sigma (Knockdown assay was performed by transfections using validated siRNAs targeting NFKB1/p50(SI02654932) from Qiagen. Negative control siRNA (AM4611) was purchased from Invitrogen. Stock solutions of lyophilized siRNA were prepared in nuclease-free water in accordance with the manufacturer's instructions (Qiagen and Invitrogen). NFKB1-expression plasmid and empty plasmid (pcDNA3, Life Technologies, Grand Island, NY) were subsequently transfected with FuGENE HD Transfection Reagent (Roche, Nutley, NJ).

Primary Cortical Neuronal Cultures and co-culture with astrocytes

Cortices were isolated from embryonic Day 3 Sprague-Dawley rats in an ice-cold medium. Briefly, the tissue was rinsed and triturated to obtain the primary neuron suspension. Primary cortical neurons were plated at a density of 3.5 ml/well (2.0 × 106 cells/ml) and were used to perform experiments at 7 d in vitro, according to the study protocol. Excitotoxicity was produced via KA treatment of the neurons at 1 nmol/L cultured, and the co-culture was performed with a transwell device and supported with astrocytes collected from Day 7 rats as described previously [16]. For the pharmaceutical manipulation,

the cultured cells were treated with 1uM of IGF-1R inhibitor, 10 M of the PI-3 kinase/Akt inhibitor LY294022 and 10uM of p38 MAPK inhibitor SB203580.

Gene transfer and virus constructs

Recombinant adeno associated virus serotype 8 (AAV2/8) was packaged (Obio, Shanghai) with the open reading frame (ORF) of human (h) IGF-1 gene downstream of the astrocyte-specific promotor, GFAP (GFAP-AAV8-hIGF-1). This construct contained the EGFP reporter gene as well under the GFAP promoter to visually detect those transfected cells. The control construct is composed of an identical shuttle vector without the hIGF-1 gene (GFAP-AAV8 -control). Animals were anesthetized (medical oxygen 3% and isoflurane 1.5%) and fixed in a stereotaxic device (RWD Instruments, Shanghai). One small hole was drilled into the skull for the Bregma reference of lateral ventricle: 2 mm posterior, 1.5 mm lateral, and a depth of 2.5 mm beneath the dura. In each case, a Hamilton syringe with an injection needle touched the associated region and virus was gradually injected into the lateral ventricle at the rate of 0.25 ul/min for a total of 2 microliters at around 8–10 minutes. All animals received one injection with a left side of the brain with either the GFAP-AAV8-hIGF-1 or the GFAP-AAV8-control construct. Animals were cared well to recover for 4 weeks to permit the viral expression in associated brain areas, followed by the TBI or sham surgery[16]. The transfection efficiency of this virus and IGF-1 expression before and after virus injection have been validated in previous reports[16].

Mouse TBI Model, qRT-PCR, western blot, and IHC

These detailed experimental procedures were performed as previously described[16]. 6–8 week-old male C57B6 mice were administered a lateral FPI as previously described[16]. These mice were obtained from our breeding colony in the Department of Medicine, University of Shanghai Medical Health, individually housed and maintained on 12-h light/dark cycles with food and water available ad libitum. All animal experiments were approved by the Animal Ethics Committees. Briefly, under anaesthesia a 1-mm craniotomy, positioned 1.5-mm right lateral and 1.5-mm posterior to bregma, was performed to create a circular window exposing the intact dura mater of the brain. A modified female Luer-Lock cap was secured over the craniotomy window by dental acrylic. The mouse was then removed from anaesthesia and attached to the fluid percussion device via the Luer-Lock. Once the mouse responded to a toe pinch, a severeintensity (320–350 kPa) fluid pulse of silicone oil generated by the fluid percussion device was delivered to the brain. Mice were resuscitated with pure oxygen post-injury if required. On resumption of spontaneous breathing, and return to pre-FPI levels of heart rate and oxygenation status, the dental acrylic caps were removed and the wound sutured closed. The qRT-PCR primers and antibodies are listed as informed.

iTRAQ labeling

Each iTRAQ reagent (Nr01, Nr02, Nr03 and Nr04 isobaric tags) was reconstituted in ethanol, and peptide samples were reconstituted in iTRAQ dissolution buffer (AB Sciex). Samples in sets of three biological replicates were labeled with the iTRAQ reagents as follows: Sham + IGF-1 with Nr01 isobaric tag, Sham + Vector with Nr02 isobaric tag, TBI + IGF-1 with Nr03 isobaric tag, and TBI + Vector with Nr04 isobaric tag.

The labeled samples were incubated for 2 h at room temperature with interval mixing (alternating 1 min static and 15 min at 1200 rpm), centrifuged at 13 500 rpm for 5 min, and pooled together into three groups each containing one biological replicate of the studied samples. These groups were handled and analyzed separately. The pooled samples were dried by vacuum centrifugation. Sample clean-up and desalting was carried out using Macro Spin Column Filters (Nest GroupInc, Southborough, MA), filtering and washing samples several times with ACN and triethylammonium bicarbonate (TEAB; Fluka, Sigma-Aldrich) buffers. The samples were dried by vacuum centrifugation for about 1 h, and stored at − 20 Celsius degree until analysis.

LC – MS/MS Analysis

The reverse phase high-performance liquid chromatography (RP-HPLC) separation was achieved on the Easy nano-LC system (Thermo Fisher Scientific) using a self-packed column (75 μm × 150 mm; 3 μm ReproSil-Pur C18 beads, 120 Å, Dr. Maisch GmbH, Ammerbuch, Germany) at a flow rate of 300 nL/min. The mobile phase A of RP-HPLC was 0.1% formic acid in water, and B was 0.1% formic acid in acetonitrile. The peptides were eluted using a gradient (2 − 90% mobile phase B) over 90 min period into a nano-ESI Orbitrap Elite mass spectrometer (Thermo Fisher Scientific). The mass spectrometer was operated in data-dependent mode with each full MS scan (m/z 300 − 1500) followed by MS/MS for the 12 most intense ions with the parameters: ≥ +2 precursor ion charge, 2 Da precursor ion isolation window, 80 first mass and 38 normalized collision energy of HCD. Dynamic Exclusion was set for 30 s. The full mass and the subsequent MS/MS analyses were scanned in the Orbitrap analyzer with R = 60000 and R = 15000, respectively.

Luciferase reporter assay

Luciferase reporter assay was performed according to a standard protocol as described previously [21]. Briefly, primary cultured neurons ($3*10^4$ cells/well) were seeded in 24-well plates in triplicate and allowed to settle for 24 h. The indicated plasmids and 1.5 ng pRL-TK Renilla plasmid were transfected using Lipofectamine 3000 Reagent (Thermo Fisher Scientific, Waltham, MA, USA, Cat. No. L3000008). At 48 h post-transfection, luciferase and Renilla signals were determined by a Dual Luciferase Reporter Assay Kit (Promega, Cat. No. E1980) according to the manufacturer's instructions as previously described.

Chromatin immunoprecipitation-qPCR (ChIP-qPCR)

Chromatin immunoprecipitation (ChIP) was performed according to the manufacture's protocol. Briefly, crosslinking was performed with 1% formalin, and the cells were lysed in SDS buffer and sonication was used to fragment the DNA. ChIP for DCP2 was performed using a Flag antibody (Sigma, SAB4301135). Eluted DNA fragments were analyzed by qPCR. The primers are listed in section 'Chromatin immunoprecipitation-qPCR' in Supplementary Material (Table S1).

JC-10 Staining

Mitochondrial membrane potential was assessed by flow cytometry using a fluorogenic dye, JC-10 (Abcam 112133; Cambridge, MA). Treated cells were loaded with JC-10 dye according to the

manufacturer's instructions with modifications: spent medium was aspirated and complete medium added to scrape cells. JC-10 solution was added at equal volume and incubated in the dark at 37 °C for 15 minutes prior to analysis. Monomeric (green) and J-aggregate (red) fluorescence were measured using the FL1 and FL2 channels, respectively. The results were analyzed following compensation for spectral overlap in six groups as mentioned above.

Assessments of motor function and cognitive performance

Motor function was evaluated at 1, 3, 5 and 7 days after TBI using the NSS method described by [22]. Briefly, neuromuscular function, including forelimb flexion, torso twisting, lateral push, hindlimb placement, and forelimb placement; performance on an inclined board; mobility; vestibulomotor function, including performance on a balance beam; and complex neuromotor functions, including performance on a beam walk, were evaluated and given a score of 0–1 or 0–2 for neuromuscular functions, 0–6 for vestibulomotor functions and 0–5 for complex neuromotor functions.

For the Morris water maze (MWM), the temperature was maintained at 25 ± 2 °C. To ensure recovery from motor deficits, hidden platform testing was performed on post-TBI Days 11–15, and visible platform testing was performed on Days 16. Mice were allowed a maximum of 120 s to look for the submerged platform. If mice failed to reach the platform by 120 s, the experimenter placed them on the platform for 15 s. There was a minimum of 5 min between each trial. The latencies for the mouse to reach the platform and time duration in other zones were recorded and analyzed using tracking device (Chromotrack 3.0, San Diego Instruments).

Statistical analysis

Results are reported as the mean ± SD for immunoblots, fluorescence experiments and PCR results. Gray levels were detected with ImageJ. Student's t test was used to compare the differences between the two groups with Prism Software 8.00 (GraphPad Software). For behavioral tests, data were expressed as the mean ± SEM. Motor and MWM data, which are continuous, were analyzed by two-way ANOVA for overall statistical significance, followed by Tukey's post hoc test for between-group comparisons. Significant differences were defined as $p < 0.05$.

Results

Serum IGF-1 is reduced after TBI

Serum IGF-1 is lower in patients with mild TBI than those with severe TBI; The serum IGF-1 content in moderate and severe TBI at each time point was significantly lower than that of the mild TBI group ($p < 0.05$). Serum Tau progressively reduced after TBI in the first week, while it began to increase on the seventh day, but it was still remaining higher than the control group at six months post injury ($p < 0.05$, Fig. 1).

Serum IGF-1 protein was significantly higher in poor outcome group (GOS 1–3) that that in good outcome group (GOS 4–5, $p < 0.05$; Fig. 1). Serum IGF-1 content at 1, 3, 5, 7, and 14 days after injury (acute and subacute stage) had a significant positive correlation with MoCA score even at 6 months after injury ($R2 = 0.2484$, $p < 0.001$).Serum IGF-1 in normal cognition group is higher than it in abnormal cognition group at acute stage of TBI patients as well (Fig. 1).

Astrocytic IGF-1 has neuroprotective role in TBI models

Previously we have shown astrocytic IGF-1 protects against excitotoxic neurons both in-vivo and in-vitro. Therefore, we used astrocytic IGF-1 to treat lateral fluid percussion injury (LFPI) mouse model (done at Shanghai Health College). Mice were tested in the water maze to assess cognitive function 12 weeks after injury. During the acquisition session of the water maze, mice given a FPI and treated with astrocytic IGF-1 displayed significantly faster search times than their vehicle-treated counterparts. There were no significant effects on the measure of crossing time and during in the targeted zone during water maze acquisition period ($P > 0.05$). Furthermore, the astrocytic IGF-1 improved both cognition and motor function in TBI mice by Morris water maze and NSS assessment (Fig. 2). TBI mice had higher NSS; while astrocytic IGF-1 could reduce it.

iTRAQ and bioinformatic analysis in IGF-1 treated TBI mice

Next, we applied iTRAQ proteomics to investigate the neuroprotective effect of astrocytic IGF-1. According to the iTRAQ method published previously, we compared the targeting proteins with a two-fold alteration in TBI vs. Sham group with vectors and TBI + IGF-1 vs. TBI + vector. We identified 189 candidate proteins after IGF-1 treatment. First, we did a David Analysis with an online tool (https://david.ncifcrf.gov) and clustered these candidate proteins based on KEGG analysis (Supp Fig. 1). We listed top 20 cluster and KEGG pathway in Fig. 3. The Top 20 Cluster pathway (David analysis)showed Hydrolase activity (GO:0016787 ~ hydrolase activity) is the first one, including 16 related proteins (Q9CYC6, Q9CR30, Q50L41, Q9R001, Q6NSR8, Q8CGB6, Q9WUZ9, Q9ET22, Q91ZX6, P35821, P52479, Q8CHE4, Q9CXY9, P97470, P07146, Q14BV6) and the top KEGG pathway is membrane protein (Table S2).

DCP2 and related pathway changes after TBI

DCP2(Q9CYC6)is found to increase in TBI group with more than 2-fold change, and IGF-1 treatment could reduce its expression by 1.4 times. Dcp2 codes m7GpppN-mRNA hydrolase in mammalians [23]. M7G is a 5'capping structure in mRNA and also in miRNA. The METTL1 (another m7G decapping enzyme) has been found to promote the maturation of several miRNAs via disrupting the immature structure for miRNA [24]. And METTL1 knockdown could reduce the expression of a serious of miRNAs including let 7e with a most decreased level [24]. Here, we predicted DCP2 is supposed to be decapping the m7G structure of let 7e as well to promote its maturation and checked the expression of DCP2 and IGF-1R in cell models.

To validate this, we did an in-vitro analysis with an excitotoxic model, which can mimic the brain injury in cells. First we observed KA treated neurons had decreased MAP2 and beta-tubulin expression indicating reduced maturation of neurons; while co-culture with astrocytes could promote the neuronal growth and against the excitotoxic effect with increased expression of both MAP2 and beta-tubulin to validate our previous findings and the successful modeling of in-vitro excitotoxic injury (Supp Fig. 2). Next, we found both DCP2 and let 7e expression increased in KA treated neurons; while coculture with astrocytes could reduce both. These findings were consistent with our TBI in vivo results. And this effect was abolished partly by IGF-1R antagonist, PI3K inhibitor and p38 inhibitor (Fig. 3).

Mir let-7e has previously been reported to regulate IGF-1R [25]. In our study, we did a Targetscan analysis for the binding prediction between IGF-1R 3'UTR and let-7e. Further, we confirmed this with luciferase assay. Next, the dual luciferase reporter gene assay with the psicheck2-based IGF-1R-wt plasmid containing miR-let-7e binding site was conducted to further verify this prediction. The activity of the luciferase following cotransfection of IGF1R-wt and miR-let-7e mimic was lower than the activity following cotransfection of IGF-1R-wt and NC ($p < 0.05$), indicating that there was a regulatory relationship between miR-let-7e and 3'-UTR of IGF-1R (Fig. 3). These findings helped to verify that miR-let-7e targeted IGF-1R.

Mitophagy of brain injury in-vitro and in-vivo

It is reported that IGF-1R can regulate the autophagy and IGF-1 can promote mitophagy via activating AMPK [11]. To confirm the IGF-1 role in mitophagy following brain injury, we did both in-vitro and in vivo analysis of mitophagy. This study further evaluated whether the increased neuronal loss in KA-stressed cells was accompanied by of a loss of mitochondrial potential and if astrocytic IGF-1 could affect this phenomenon. The cells were analyzed with the JC-10 dye that forms red J-aggregates in controlled primary cultured cells but stays a green monomer in cells that have lost mitochondrial integrity. The scatter plots show that majority of the cells treated with KA shifted towards green fluorescence when compared to controls (Fig. 4). Remarkably, in KA treated neurons cocultured with astrocytes, a population shift to the red channel was observed indicating preservation of mitochondrial potential. In addition, this effect was partly abolished by IGF-1R antagonist, PI3K inhibitor and p38 inhibitor. Consequently, KA-stressed cells maintained mitochondrial potential when cocultured with astrocytic IGF-1 (Fig. 4).

In addition, we extracted the mitochondria proteins from the cultured cell to assess the mitophagy following KA. We found KA increased the expression of Atg8, Atg 5, Atg 14, Beclin-1and Lamp while decreased the p62SQSTM1 level. This effect is partly abolished by AG1024, PI3K inhibitor and p38 MAPK inhibitor (Fig. 5).

For the in-vivo study, we applied the IHC to analyze the mitophagy marker (PINK1 and NIX) in the rodent TBI brain. As shown in Fig. 6, FPI in mice induced the decreased NIX and PINK1 expression (shown as average optical density of brown area) in the ipsilateral cortex of TBI mice at three months after injury and IGF-1 treatment could reverse these.

Discussion

In the present study, we applied iTRAQ proteomics to demonstrate a subset of proteins changed in TBI and reversed by genetic manipulation of astrocytic IGF-1. The pathway analysis showed hydrolysis lied at the top in the cluster. We identified Dcp2, a m7G hydrolysis increased after TBI and decreased by IGF-1 treatment. Further, we found astrocytic IGF-1 could also reverse the interrupted mitophagy after TBI. Mechanical study demonstrated Dcp2 could promote the mature of let-7 family and further decrease the IGF-1R and related mitophagy. Based on these findings, we proposed an orchestration between IGF-1 and IGF-1R to facilitate the mitophagy after TBI.

IGF-1/IGF-1R and miR-let-7e have been previously reported to down-regulate each other and modulate proliferation and migration in colorectal cancer cells. The author also found let-7e could reduce the expression of IGF-1R with qPCR test, and IGF-1 treatment was able to decrease the expression of let-7e as well. However, the authors did not further investigate the mechanisms[26]. In our report, we applied the luciferase assay to link the let-7e and IGF-1R, and proteomic method to identify the mechanism behind how IGF-1 reduced let-7e with a m7G decapping mechanism.

The presence of m7G in miRNAs strongly indicates a new RNA methylated regulation in non-coding RNAs. And this might exist in long non-coding RNAs (LncRNAs). Previous study has identified G-quadruplex structure is known to be inhibitory to miRNA processing [27], and the G-quadruplex motif in let-7e overlaps the DROSHA cleavage site. Therefore, we proposed that Dcp2-mediated deposition of m7G within G-rich regions destabilizes G-quadruplexes, thereby promoting their processing from pri- to pre-miRNA (Supp Fig. 6). Sarah et al reported that many lncRNAs are degraded by DCP2 [28]and a recent article has identified the catalytic structure of DCP2 [29]. It has also reported that DCP2 decapping enzyme is redundant and required for miRNA-mediated gene silencing [23], consistent in our studies, DCP2 might facilitate the maturation of miRNA to carry out the gene silencing function. More importantly, DCP2 level is supposed to affect the let-7 expression [30].

Removal of the 5' cap on mRNA by the decapping enzyme Dcp2 is a critical step in 5'-to-3' mRNA decay. However, recent report found the m7G methylation might promotes miRNA processing with METTL1, a major Methyltransferase. In such, Dcp2 could decay mRNAs via facilitating their associated miRNA. And the accumulation of miRNA targets increased concomitantly with the decrease of miRNA in the decapping mutants [31]. Therefore, we proposed that the increased Dcp2 after brain injury could facilitate the expression of miRNA and reduce the targeted mRNAs. Sarah et al reported that many lncRNAs are degraded by DCP2 [28]and a recent article has identified the catalytic structure of DCP2 [29].

Previous studies have shown IGF-1 can regulate exosome-mediated miRNAs transfer and maintain the tumor cell proliferation [32]. IGF-1 from tumor initiating cells can prevent miR-122 production in neighboring normal hepatocytes and thereby curtail its intercellular transfer within exosome, leading to low levels of the anti-proliferative miRNAs in hepatic cancer cells. However, the author did not investigate the mechanism how IGF-1 regulated the miR-122 expression [33]. This finding is consistent with our study and we further found that IGF-1 could regulate the miRNA expression through m7G hydrolysis with our

proteomics data. Another study shows macrophages can release IGF-1 influence its phagocyte ability and inflammation. The IGF-1 from macrophages can bind to the surface of non-professional phagocytes (such as epithelial cells). Meanwhile, IGF-1 could enhance the uptake of macrovesicles for epithelial cells and deletion of IGF-1 receptor led to exacerbated inflammation [34]. Therefore, it would be interesting in our future study to investigate how astrocytic IGF-1 influence the exosomes release and neuronal phenotype. In addition, exosomes are full of non-coding RNAs including both miRNAs and lncRNAs, which could be indirectly regulated by IGF-1 as well.

As previously reported, exogenous IGF-1 sustains cell viability in cancer cell lines by stimulating mitochondrial biogenesis and BNIP3-induced mitophagy [35], and IGF-1 can also augment mitochondrial function and neuronal metabolism via AMPK [11]. However, no previous study has linked the IGF-1 and neuronal mitophagy in brain insults. As tau phosphorylation can further impair the autophagy pathway and astrocytic IGF-1 could reduce the phosphor-tau both in vivo and in vitro [16] (Supp Fig. 3), we proposed that IGF-1 could promote the mitophagy and downregulate p-tau in a beneficial circle. This is consistent with previous study that both impaired mitophagy and p-tau form a vicious circle to aggravate neurodegeneration by affecting each other [36]. We found KA treated neurons had increased mitophagy level, decreased mitochondrial membrane potential (JC-10 staining) and autophagosomes (p62 expression) while cocultured astrocytes could reverse these with IGF-1 pathway dependent. These findings are consistent with previous studies [37, 38]. This is important in our study that IGF-1 is able to affect both pathways and improve neurological outcome after brain injury. In addition, in our proteomics study, we also found TBI reduced the expression of ATIF1 (a mitochondrial ATPase inhibitor) and ATPase delta subunit, while the astrocytic IGF-1 could reverse these (unpublished data). ATIF1 is reported to be a risk factor in AD patients with decreased expression ATIF1 in a single-cell seq study [39]. This might explain the mechanism how mitophagy impaired after TBI. In our in-vitro study, we also found the facilitation of mitophagy induced by IGF-1 is partly abolished by IGF-1R antagonist, PI-3K inhibitor and p38 blocker. This indicates the impaired mitophagy is due to the dysregulated IGF-1-PI3K-NF-kB pathway. We found TBI can activate the NF-KB pathway and astrocytic IGF-1 deactivate the NF-kB by KEGG pathway analysis (Supp Fig. 1). mTOR inhibitor has also been found to increase mitophagy in TBI via activating the IGF-1-PI3K signaling pathway. Meanwhile, after a prediction from Autophagy Regulatory Network, we found there might be a relationship between Nfkb1 and Dcp2 (Supp Fig. 4). And this transcriptional regulation of protein-DNA association was also predicted from JASPAR database (Supp Fig. 4), and the correlational study between DCP2 and NFKB1 from GEPIA Tool showing the expression in hippocampus showing they have a positive correlation with a R value at 0.69 (http://gepia.cancer-pku.cn/detail.php) further confirm this (Supp Fig. 5). In our findings, Dcp2 increased in excitotoxic neurons and co-cultured astrocytes could reverse this (Fig. 3). This effect was partly abolished by IGF-1R antagonist, PI3K inhibitor and p38 inhibitor. We further did a chip-qPCR and luciferase assay report to demonstrate the transcriptional regulation effect between NFKB1 and DCP2 (Supp Fig. 5). Therefore, it is confirmed that NF-KB pathway might regulate the transcription of Dcp2, and the role of this regulation in TBI session needs to be validated in future studies.

Many mechanisms control cell proliferation, and one of the most important drivers is the PI3k-AKT signaling pathway [40]. Notably, METTL1, one of the major m7G decapping enzyme, can be phosphorylated by AKT directly and its activity is inhibited aftermost [41]. Given the findings presented here, it is likely that the hypofunction of AKT in TBI would increase the levels of m7G-containing miRNAs, including the let-7 family. This family in particular inhibits the progression and invasiveness of numerous tumors, including lung cancer, by regulating the expression of key oncogenes such as RAS, MYC, and HMGA2 [42]. The control of let-7 family members by the m7G pathway may represent a common mechanism to modulate their expressions and activities. Beyond cancer, let-7 is also implicated in neurodegenerative diseases, such as Alzheimer's disease, in which it is significantly upregulated [43]. Furthermore, low levels of let-7 have been shown to improve tissue repair through reprogramming cellular metabolism [44, 45]. Therefore, direct targeting of IGF-1/IGF-1R could represent a valid and unexplored therapeutic strategy in these pathological contexts. This report identifies the IGF-1 through m7G pathway as a novel regulator of miRNA function and further affects the IGF-1R to orchestrate the mitophagy after brain insults. Considering the interest in miRNA and lncRNA targets and tools in therapeutic intervention [46], our findings could be exploited in many non-coding RNAs-related disease settings to open up new therapeutic avenues.

Conclusion

In our study, we found astrocytic IGF-1 regulates miR-let 7e through DCP2 and further affects IGF-1R to orchestrate mitophagy in TBI. Astrocytic IGF-1/IGF-1R might affect the maturation of non-coding RNAs to facilitate mitophagy and improve neurological outcomes after brain insults.

Abbreviations

A mitochondrial ATPase inhibitor (ATIF1)

Chromatin immunoprecipitation (ChIP)

Decapping mRNA2 (Dcp2)

Glial factor (GFAP)

Glasgow Coma Scale (GCS)

Glasgow Outcome Scale GOS)

Glycogen synthesis kinase (GSK)3β

Growth factor (GH)

Insulin-like growth factor 1 (IGF-I)

Insulin-like growth factor 1 Receptor (IGF-1R)

Kainic acid (KA)

Long non-coding RNAs (LncRNAs)

Mitogen-activated protein kinase (MAPK)

Mass Spectroscopy (MS)

Microtubule associated protein (MAP)

Montreal Cognition Assessment (MoCA)

Methyltransferase Like 1 (METTL1)

Morris water maze (MWM)

Thiazolyl blue tetrazolium bromide (MTT)

Traumatic brain injury (TBI)

Declarations

- Ethical Approval and Consent to participate

No clinical data are included in the manuscript.

- Consent for publication

All authors agree to publish the current manuscript.

- Availability of supporting data

The iTRAQ data are available in the supplementary files.

- Competing interests

The authors declare that they have no competing interests.

- Funding

This work was supported by National Scientific Foundation of China (81701231) to Ping Zheng, National Scientific Foundation of Shanghai (16ZR1431500) to Ping Zheng; Also Interdisciplinary Program of Shanghai Jiao Tong University (ZH2018QNB01), Clinical Research Program of Ninth People's Hospital affiliated to Shanghai Jiao Tong University School of Medicine (JYZZ029) to Liang Shu.

- Authors' contributions

ZP & LS conceived, designed the experiments, RDB and CW performed cell cultures. CW and LS ran the molecular tests. CK, WZH wrote the manuscript. All authors read and approved the final manuscript. All authors read and approved the final manuscript.

- Acknowledgements

Not applicable.

- Authors' information

Not applicable.

References

1. GBD 2016 Traumatic Brain Injury and Spinal Cord Injury Collaborators. Global, regional, and national burden of traumatic brain injury and spinal cord injury, 1990–2016: a systematic analysis for the Global Burden of Disease Study 2016. Lancet Neurol. 2019;18:56–87.
2. Ma H-P, Chen P-S, Wong C-S, Chang C-F, Ou J-C, Tsai Y-R, et al. Psychometric Evaluation of Anxiety, Depression, and Sleep Quality after a Mild Traumatic Brain Injury: A Longitudinal Study. Behav Neurol. Hindawi; 2019;2019:4364592–9.
3. Shultz SR, Wright DK, Zheng P, Stuchbery R, Liu S-J, Sashindranath M, et al. Sodium selenate reduces hyperphosphorylated tau and improves outcomes after traumatic brain injury. Brain. 2015;138:1297–313.
4. Liu S-J, Zheng P, Wright DK, Dezsi G, Braine E, Nguyen T, et al. Sodium selenate retards epileptogenesis in acquired epilepsy models reversing changes in protein phosphatase 2A and hyperphosphorylated tau. Brain. 2016;139:1919–38.
5. Tan XL, Zheng P, Wright DK, Sun M, Brady RD, Liu S, et al. The genetic ablation of tau improves long-term, but not short-term, functional outcomes after experimental traumatic brain injury in mice. Brain Inj Taylor Francis. 2019;29:1–9.
6. Zheng P, He B, Tong WS. Decrease in pituitary apparent diffusion coefficient in normal appearing brain correlates with hypopituitarism following traumatic brain injury. J Endocrinol Invest Springer International Publishing. 2014;37:309–12.
7. Zheng P, He B, Guo Y, Zeng J, Tong W. Decreased apparent diffusion coefficient in the pituitary and correlation with hypopituitarism in patients with traumatic brain injury. J Neurosurg American Association of Neurological Surgeons. 2015;123:75–80.
8. Zheng P, He B, Tong W. Dynamic pituitary hormones change after traumatic brain injury. Neurol India. 2014;62:280–4.

9. Arwert LI, Deijen JB, Müller M, Drent ML. Long-term growth hormone treatment preserves GH-induced memory and mood improvements: a 10-year follow-up study in GH-deficient adult men. Horm Behav. 2005;47:343–9.
10. Feeney C, Sharp DJ, Hellyer PJ, Jolly AE, Cole JH, Scott G, et al. Serum insulin-like growth factor-I levels are associated with improved white matter recovery after traumatic brain injury. Ann Neurol. 2017;82:30–43.
11. Aghanoori M-R, Smith DR, Shariati-Ievari S, Ajisebutu A, Nguyen A, Desmond F, et al. Insulin-like growth factor-1 activates AMPK to augment mitochondrial function and correct neuronal metabolism in sensory neurons in type 1 diabetes. Mol Metab. 2019;20:149–65.
12. Chen H, Chan YL, Nguyen LT, Mao Y, de Rosa A, Beh IT, et al. Moderate traumatic brain injury is linked to acute behaviour deficits and long term mitochondrial alterations. Clin. Exp. Pharmacol. Physiol. John Wiley & Sons, Ltd (10.1111); 2016;43:1107–14.
13. Yin Y, Li E, Sun G, Yan HQ, Foley LM, Andrzejczuk LA, et al. Effects of DHA on Hippocampal Autophagy and Lysosome Function After Traumatic Brain Injury. Mol Neurobiol. 2018;55:2454–70.
14. Cummins N, Tweedie A, Zuryn S, Bertran-Gonzalez J, Götz J. Disease-associated tau impairs mitophagy by inhibiting Parkin translocation to mitochondria. EMBO J. 2019;38:71.
15. Chen W, He B, Zheng P. Astrocytic insulin-like growth factor-1 prevents excitotoxic downregulation of adenosine deaminase acting on RNA in calcium dynamics. J. Cell. Biochem. John Wiley & Sons, Ltd; 2019;120:9097–103.
16. Chen W, He B, Tong W, Zeng J, Zheng P. Astrocytic Insulin-Like Growth Factor-1 Protects Neurons Against Excitotoxicity. Front Cell Neurosci Frontiers. 2019;13:298.
17. Madathil SK, Carlson SW, Brelsfoard JM, Ye P, D'Ercole AJ, Saatman KE. Astrocyte-Specific Overexpression of Insulin-Like Growth Factor-1 Protects Hippocampal Neurons and Reduces Behavioral Deficits following Traumatic Brain Injury in Mice. Schmidt MV, editor. PLoS ONE. Public Library of Science; 2013;8:e67204.
18. Frenette LC, Tinawi S, Correa JA, Alturki AY, LeBlanc J, Feyz M, et al. Early detection of cognitive impairments with the Montreal Cognitive Assessment in patients with uncomplicated and complicated mild traumatic brain injury. Brain Inj. 2nd ed. Taylor & Francis; 2018;33:1–9.
19. Waldron-Perrine B, Gabel NM, Seagly K, Kraal AZ, Pangilinan P, Spencer RJ, et al. Montreal Cognitive Assessment as a screening tool: Influence of performance and symptom validity. Neurol Clin Pract. 2019;9:101–8.
20. Panwar N, Purohit D, Deo Sinha V, Joshi M. Evaluation of extent and pattern of neurocognitive functions in mild and moderate traumatic brain injury patients by using Montreal Cognitive Assessment (MoCA) score as a screening tool: An observational study from India. Asian J Psychiatr. 2019;41:60–5.
21. Zheng P, Bin H, Chen W. Inhibition of microRNA-103a inhibits the activation of astrocytes in hippocampus tissues and improves the pathological injury of neurons of epilepsy rats by regulating BDNF. Cancer Cell Int BioMed Central. 2019;19:109–14.

22. Xiong Y, Mahmood A, Chopp M. Animal models of traumatic brain injury. Nat Rev Neurosci Nature Publishing Group. 2013;14:128–42.
23. Rehwinkel J, Behm-Ansmant I, Gatfield D, Izaurralde E. A crucial role for GW182 and the DCP1:DCP2 decapping complex in miRNA-mediated gene silencing. RNA Cold Spring Harbor Lab. 2005;11:1640–7.
24. Pandolfini L, Barbieri I, Bannister AJ, Hendrick A, Andrews B, Webster N, et al. METTL1 Promotes let-7 MicroRNA Processing via m7G Methylation. Mol. Cell. 2019;74:1278–9.
25. Kumar AS, Rayala SK, Venkatraman G. Targeting IGF1R pathway in cancer with microRNAs: How close are we? RNA Biol Taylor Francis. 2018;15:320–6.
26. Li Z, Pan W, Shen Y, Chen Z, Zhang L, Zhang Y, et al. IGF1/IGF1R and microRNA let-7e down-regulate each other and modulate proliferation and migration of colorectal cancer cells. Cell Cycle Taylor Francis. 2018;17:1212–9.
27. Mirihana Arachchilage G, Morris MJ, Basu S. A library screening approach identifies naturally occurring RNA sequences for a G-quadruplex binding ligand. Chem Commun (Camb) The Royal Society of Chemistry. 2014;50:1250–2.
28. Geisler S, Lojek L, Khalil AM, Baker KE, Coller J. Decapping of long noncoding RNAs regulates inducible genes. Mol Cell. 2012;45:279–91.
29. Mugridge JS, Tibble RW, Ziemniak M, Jemielity J, Gross JD. Structure of the activated Edc1-Dcp1-Dcp2-Edc3 mRNA decapping complex with substrate analog poised for catalysis. Nat Commun Nature Publishing Group. 2018;9:1152–10.
30. Li Y, Song M, Kiledjian M. Differential utilization of decapping enzymes in mammalian mRNA decay pathways. RNA Cold Spring Harbor Lab. 2011;17:419–28.
31. Motomura K, Le QT, Kumakura N, Fukaya T, Takeda A, Watanabe Y. The role of decapping proteins in the miRNA accumulation in Arabidopsis thaliana. RNA Biol. Taylor & Francis; 2012;9:644–52.
32. Li S, Yao J, Xie M, Liu Y, Zheng M. Exosomal miRNAs in hepatocellular carcinoma development and clinical responses. J Hematol Oncol. 2018;11:54.
33. Basu S, Bhattacharyya SN. Insulin-like growth factor-1 prevents miR-122 production in neighbouring cells to curtail its intercellular transfer to ensure proliferation of human hepatoma cells. Nucleic Acids Res. 2014;42:7170–85.
34. Han CZ, Juncadella IJ, Kinchen JM, Buckley MW, Klibanov AL, Dryden K, et al. Macrophages redirect phagocytosis by non-professional phagocytes and influence inflammation. Nature. 2016;539:570–4.
35. Lyons A, Coleman M, Riis S, Favre C, O'Flanagan CH, Zhdanov AV, et al. Insulin-like growth factor 1 signaling is essential for mitochondrial biogenesis and mitophagy in cancer cells. J Biol Chem American Society for Biochemistry Molecular Biology. 2017;292:16983–98.
36. Feng Q, Luo Y, Zhang X-N, Yang X-F, Hong X-Y, Sun D-S, et al. MAPT/Tau accumulation represses autophagy flux by disrupting IST1-regulated ESCRT-III complex formation: a vicious cycle in Alzheimer neurodegeneration. Autophagy. Taylor & Francis; 2019;:1–18.

37. Dong XX, Wang YR, Qin S, Liang ZQ, Liu BH, Qin ZH, et al. p53 mediates autophagy activation and mitochondria dysfunction in kainic acid-induced excitotoxicity in primary striatal neurons. Neuroscience. 2012;207:52–64.
38. Zhang Y, Zhang M, Zhu W, Yu J, Wang Q, Zhang J, et al. Succinate accumulation induces mitochondrial reactive oxygen species generation and promotes status epilepticus in the kainic acid rat model. Redox Biol. 2020;28:101365.
39. Mathys H, Davila-Velderrain J, Peng Z, Gao F, Mohammadi S, Young JZ, et al. Single-cell transcriptomic analysis of Alzheimer's disease. Nature Nature Publishing Group. 2019;570:332–7.
40. Li Z, Gao W, Fei Y, Gao P, Xie Q, Xie J, et al. NLGN3 promotes neuroblastoma cell proliferation and growth through activating PI3K/AKT pathway. Eur J Pharmacol. 2019;857:172423.
41. Cartlidge RA, Knebel A, Peggie M, Alexandrov A, Phizicky EM, Cohen P. The tRNA methylase METTL1 is phosphorylated and inactivated by PKB and RSK in vitro and in cells. EMBO J. 2005;24:1696–705.
42. Balzeau J, Menezes MR, Cao S, Hagan JP. The LIN28/let-7 Pathway in Cancer. Front Genet. 2017;8:31.
43. Gu H, Li L, Cui C, Zhao Z, Song G. Overexpression of let-7a increases neurotoxicity in a PC12 cell model of Alzheimer's disease via regulating autophagy. Exp Ther Med Spandidos Publications. 2017;14:3688–98.
44. McDaniel K, Hall C, Sato K, Lairmore T, Marzioni M, Glaser S, et al. Lin28 and let-7: roles and regulation in liver diseases. Am J Physiol Gastrointest Liver Physiol. 2016;310:G757–65.
45. McDaniel K, Huang L, Sato K, Wu N, Annable T, Zhou T, et al. The let-7/Lin28 axis regulates activation of hepatic stellate cells in alcoholic liver injury. J Biol Chem. 2017;292:11336–47.
46. Chakraborty S, Andrieux G, Hasan AMM, Ahmed M, Hosen MI, Rahman T, et al. Harnessing the tissue and plasma lncRNA-peptidome to discover peptide-based cancer biomarkers. Sci Rep Nature Publishing Group. 2019;9:12322–17.

Figures

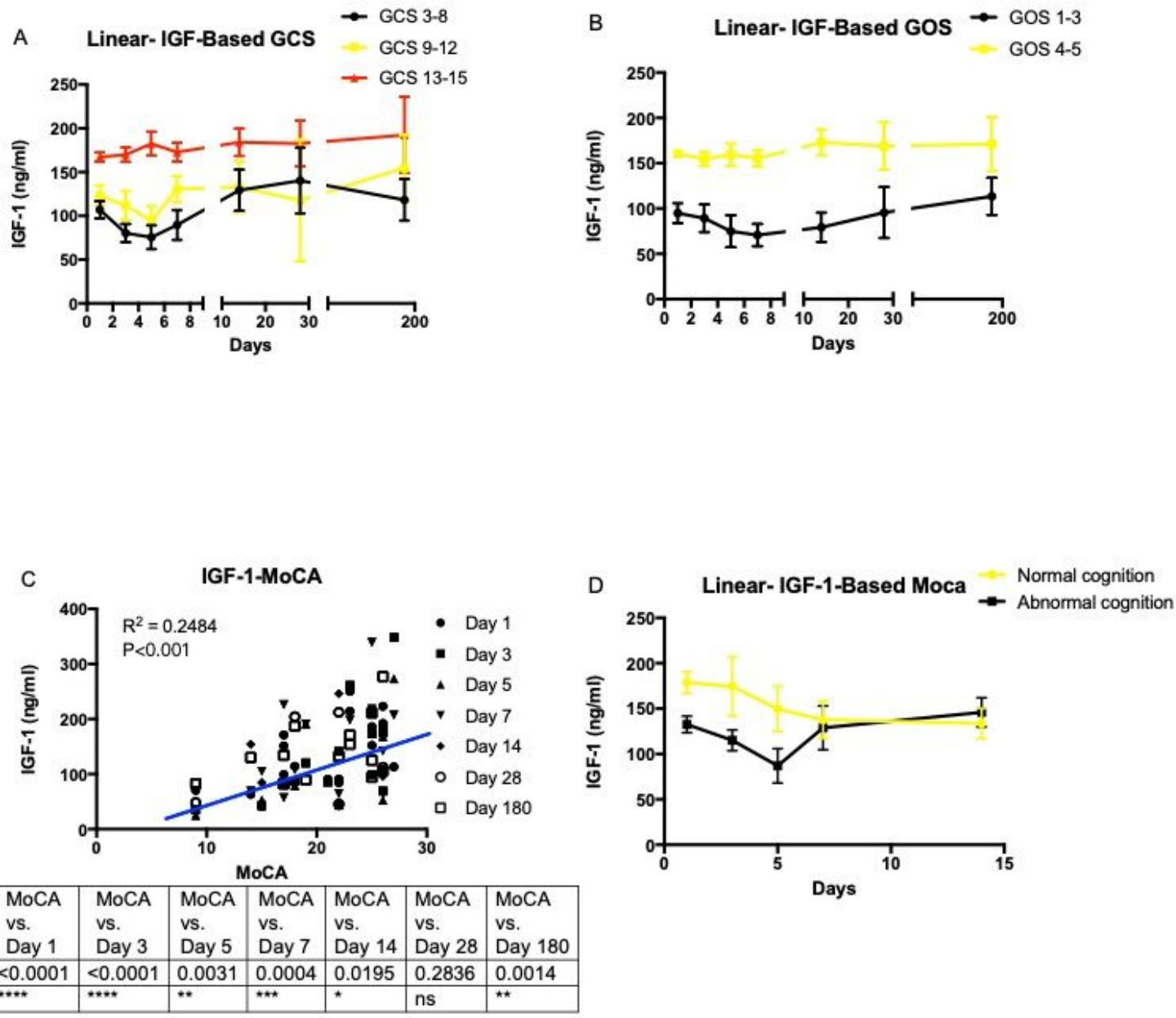

MoCA vs. Day 1	MoCA vs. Day 3	MoCA vs. Day 5	MoCA vs. Day 7	MoCA vs. Day 14	MoCA vs. Day 28	MoCA vs. Day 180
<0.0001	<0.0001	0.0031	0.0004	0.0195	0.2836	0.0014
****	****	**	***	*	ns	**

Figure 1

The correlation between dynamic serum IGF-1 and GCS, GOS and MoCA. Fig A, Serum IGF-1 is lower in patients with mild TBI than those with severe TBI; Fig B，Serum IGF-1 in good outcome group（GOS4-5）is higher than it in poor outcome group（GOS1-3）;Fig C，Serum IGF-1 is positively associated with MoCA score（r2=0.775，p<0.05）;Fig D，Serum IGF-1 in normal cognition group is higher than it in abnormal cognition group.

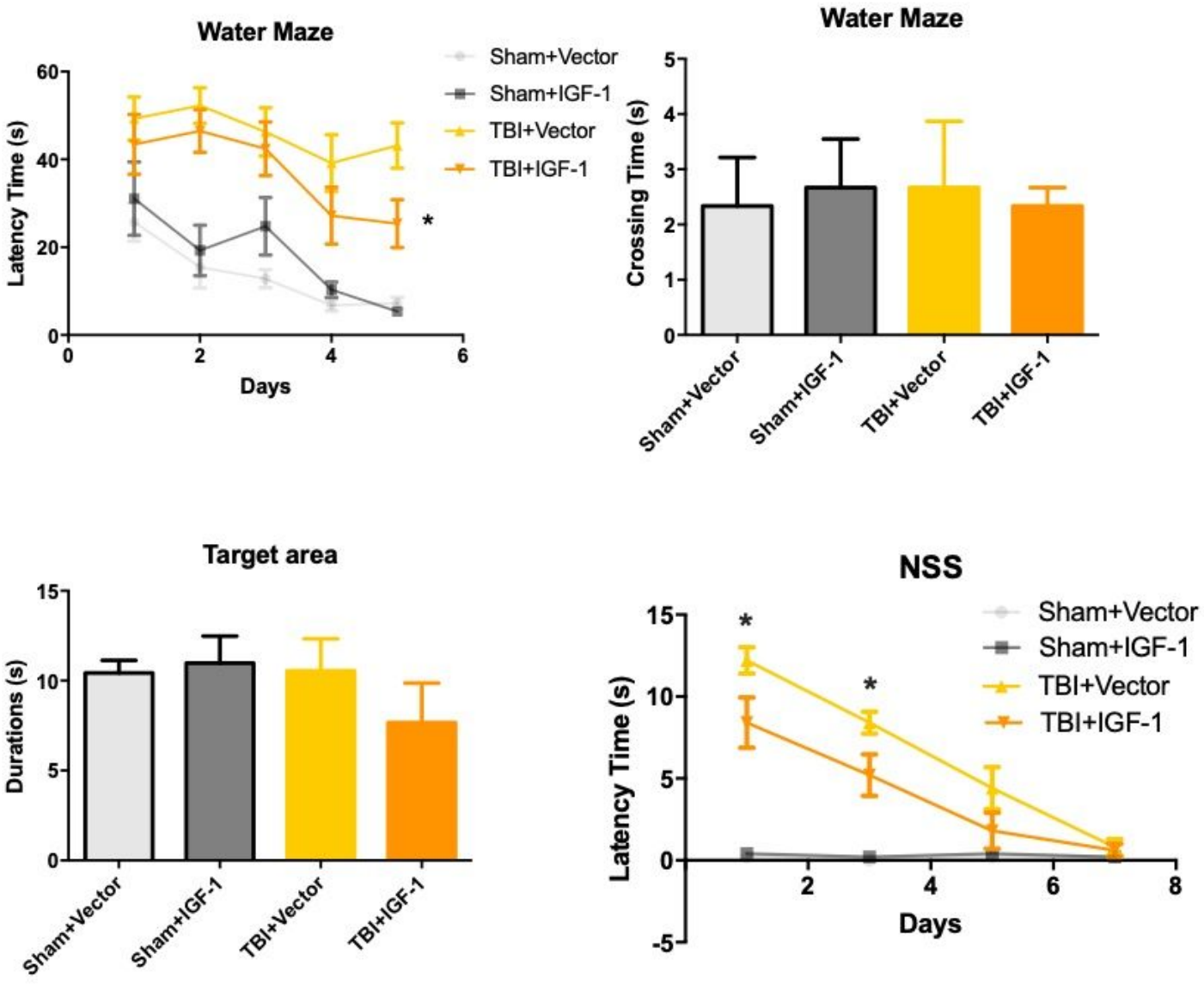

Figure 2

Astrocytic IGF-1 reduces cognitive and motor impairments after TBI.Mice given a FPI and treatedwith vector had longer search times in the water maze, whereas TBI micetreated with astrocytic IGF-1 displayed fewer search time. There is no difference in crossing time and durations among the groups. As for the motor function, TBI mice with vectors have higher NSS scores and astrocytic IGF-1 could reduce the NSS. *TBI groups significantly different than sham groups, P<0.05.

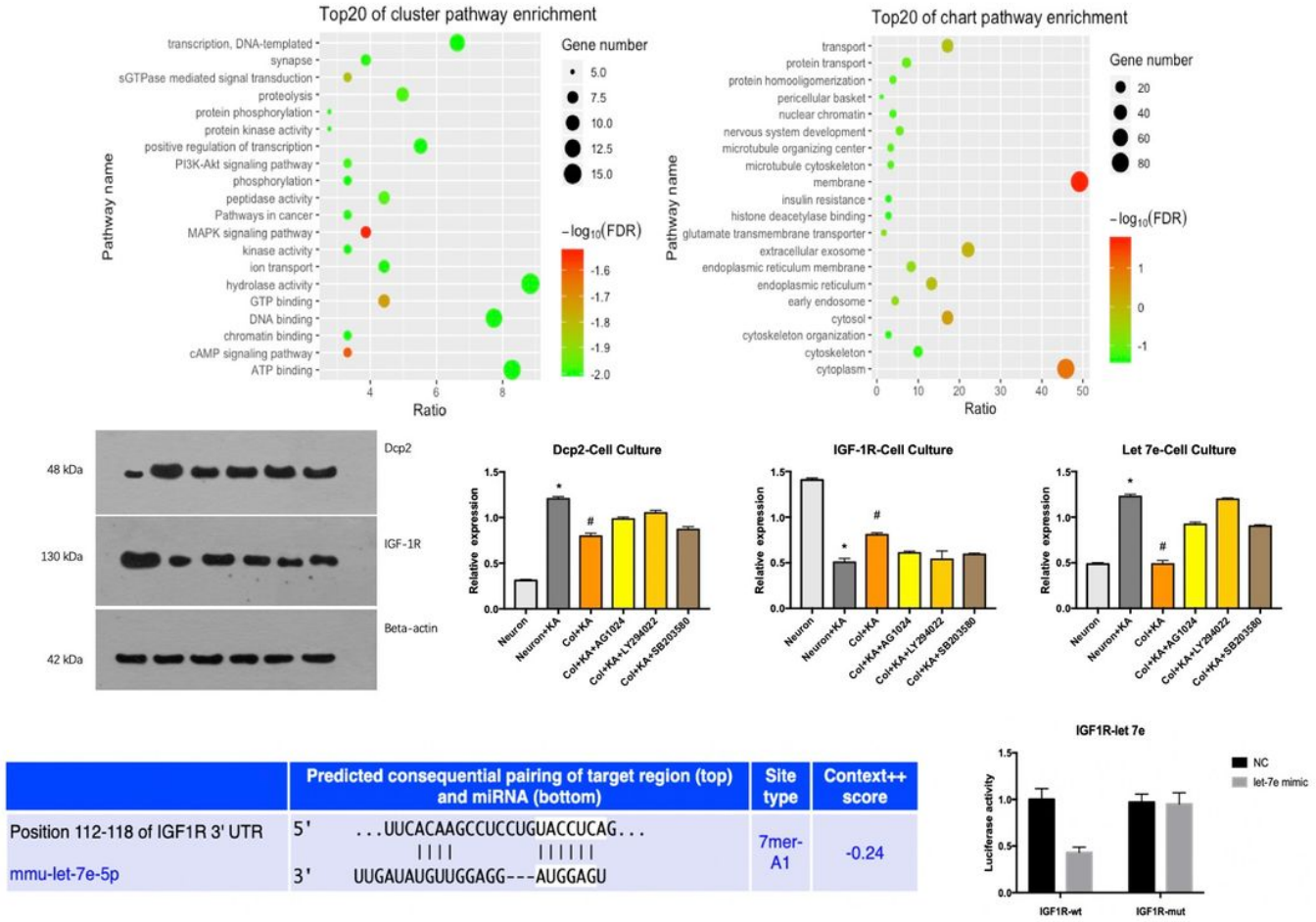

	Predicted consequential pairing of target region (top) and miRNA (bottom)	Site type	Context++ score
Position 112-118 of IGF1R 3' UTR	5' ...UUCACAAGCCUCCUGUACCUCAG...	7mer-A1	-0.24
mmu-let-7e-5p	3' UUGAUAUGUUGGAGG---AUGGAGU		

Figure 3

Pathway enrichment shows hydrolase activity and Dcp2 change after brain insults. In-vitro study shows Dcp2 and miR let-7e increase in KA treated neurons and cocultured astrocytes could reduce these with IGF-1 pathway dependent. Brain IGF-1R decreases in KA treated neurons and cocultured astrocytes could reverse this. IGF-1R is also identified as a targetgene of miR let-7e. Putative miR let-7e.binding sites in IGF-1R 3'-UTR; Luciferaseactivity of IGF-1R-wt 3'-UTR aftertransfection with miR-326 mimic; *p < .05compared with cotransfection of IGF-1R-wtand miR let-7e NC. NC,negative control; wt, wild type; mut, mutation. * KA neurons vs. neurons, p<0.05; # versus KA neurons, p<0.05.

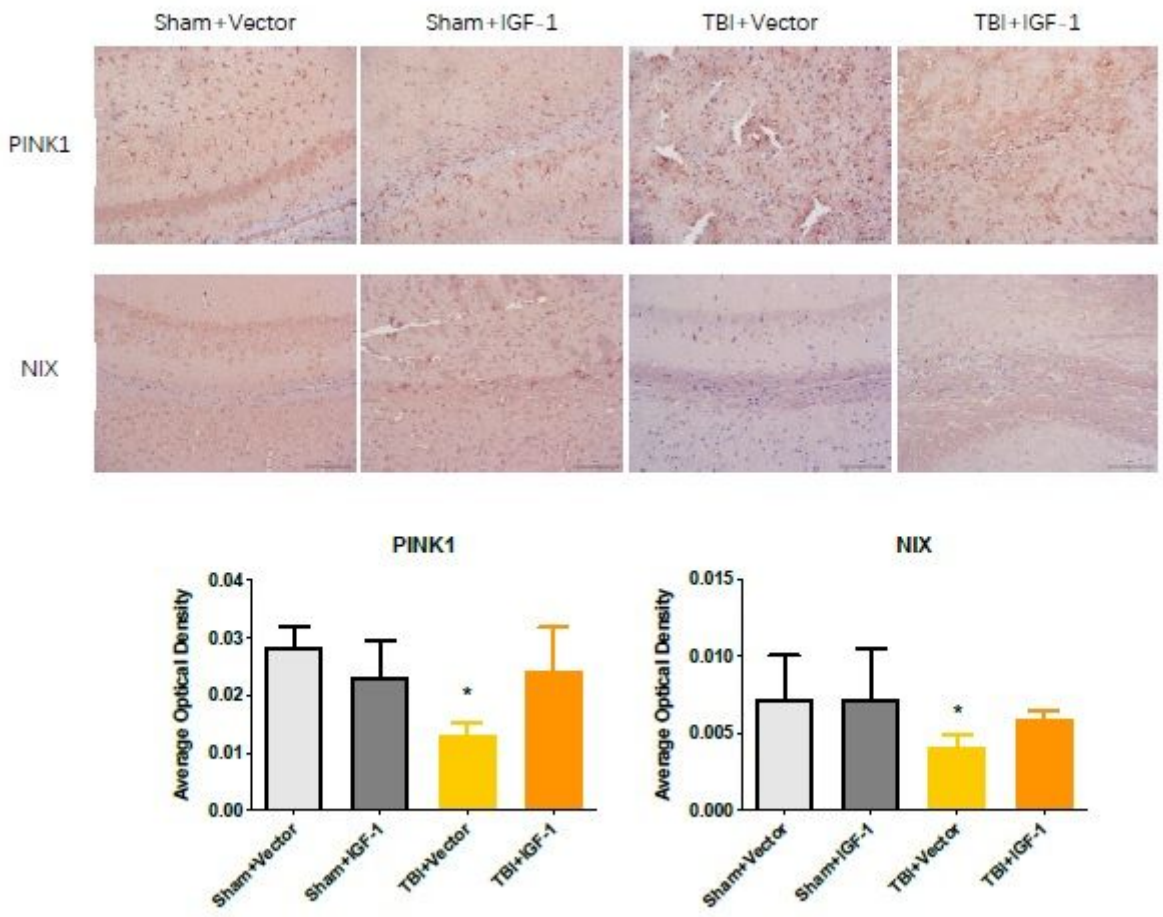

Figure 4

Cocultured astrocytes represses mitochondrial membrane disruption with IGF-1 dependent. KA treated neurons showed decreased mitochondrial membrane potential indicative of decreased Q2 (RPE level); while cocultured astrocytes could increase this. This effect was partly abolished by IGF-1R and PI3K inhibitor, but not p38 MAPK inhibitor. * KA neurons vs. neurons, $p<0.05$; # versus KA neurons, $p<0.05$.

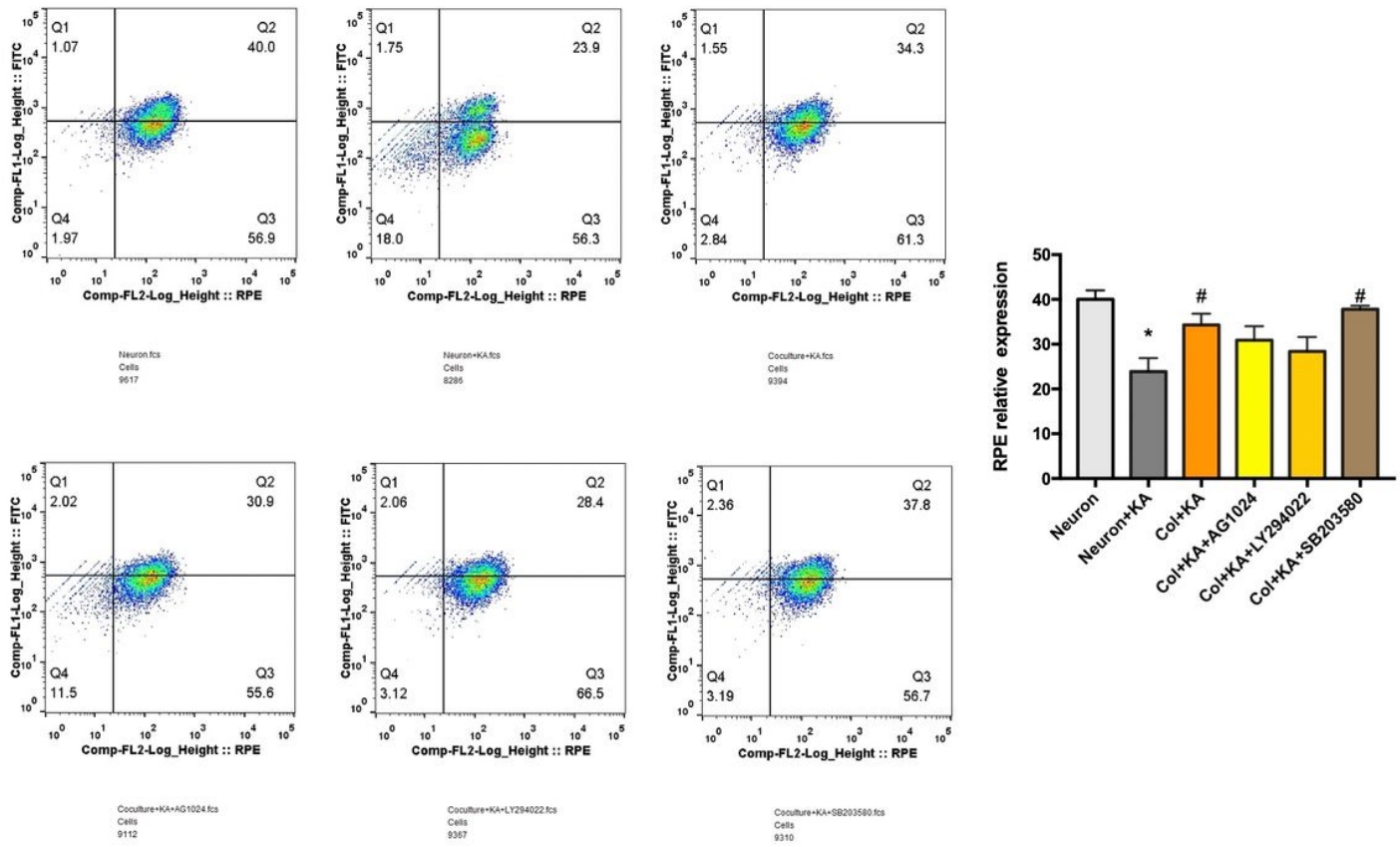

Figure 5

Activation of autophagy by KA. Expression of LC3/Atg8, Atg5, Atg14, Beclin-1 and Lamp1 increase in primary neurons treated with KA (1 μM). Expression of p62 decreased after KA. Both changes are reversed by cocultured astrocytes and this effect is differently abolished by AG1024, LY294022 and SB203580. β-actin was used as loading control. * KA neurons vs. neurons, $p<0.05$; # versus KA neurons, $p<0.05$.

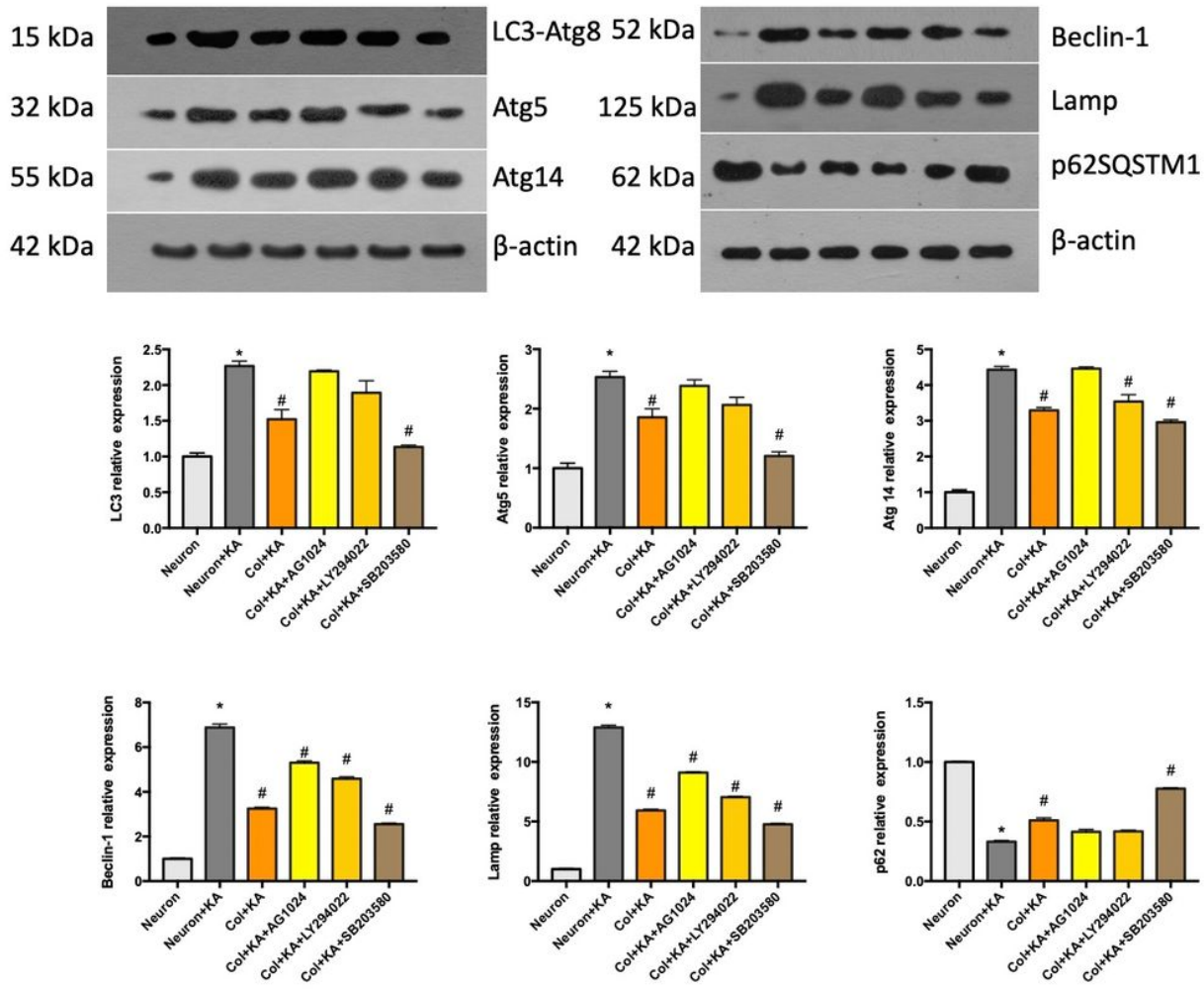

Figure 6

Dysregulated mitophagy in chronic stage of TBI. Proteinexpression of PINK1 and NIX are reduced at three months post injury, IGF-1 treatment could increase both. *. P<0.05, compared to other groups.

Supplementary Files

This is a list of supplementary files associated with this preprint. Click to download.

- SuppTable2.xlsx
- SuppTable1.xlsx
- SuppforNeurology1.pdf